Journal of Magnetic Resonance **141,** 34–43 (1999)
Article ID jmre.1999.1881, available online at http://www.idealibrary.com on IDEAL®

MUSIC in Triple-Resonance Experiments: Amino Acid Type-Selective ^{1}H–^{15}N Correlations

Mario Schubert, Maika Smalla, Peter Schmieder,[1] and Hartmut Oschkinat

Forschungsinstitut für Molekulare Pharmakologie, Alfred-Kowalke-Strasse 4, D-10315 Berlin, Germany

Received March 22, 1999; revised July 14, 1999

Amino acid type-selective triple-resonance experiments can be of great help for the assignment of protein spectra, since they help to remove ambiguities in either manual or automated assignment procedures. Here, modified triple-resonance experiments that yield amino acid type-selective ^{1}H–^{15}N correlations are presented. They are based on novel coherence transfer schemes, the MUSIC pulse sequence elements, that replace the initial INEPT transfer and are selective for XH_2 or XH_3 (X can be ^{15}N or ^{13}C). The desired amino acid type is thereby selected based on the topology of the side chain. Experiments for Gly (G-HSQC); Ala (A-HSQC); Thr, Val, Ile, and Ala (TAVI-HSQC); Thr and Ala (TA-HSQC), as well as Asn and Gln (N-HSQC and QN-HSQC), are described. The new experiments are recorded as two-dimensional experiments and therefore need only small amounts of spectrometer time. The performance of the experiments is demonstrated with the application to two protein domains.

Key Words: **triple resonance; proteins; editing; HSQC; assignment.**

INTRODUCTION

For the investigation of structure and dynamics of proteins by NMR a sequence-specific assignment of the resonances of all NMR-active nuclei is a prerequisite. This crucial step has been facilitated by the introduction of triple-resonance experiments (*1, 2*) that allow for an assignment of resonances from proteins with a molecular weight of less than 20 kDa in a straightforward manner. These techniques yield spectra with high sensitivity and good intrinsic resolution and use magnetization pathways that are independent of the three-dimensional structure of the protein. Therefore, the corresponding spectra are supposed to be ideally suited for an automation of the assignment procedure (*3–8*). Independent of whether the assignment is done manually or in an automated fashion, the starting point will usually be a ^{15}N-HSQC spectrum, which contains a "fingerprint" of the protein, i.e., a pair of (^{1}H, ^{15}N) frequencies for each residue. These frequencies also occur in those three-dimensional triple-resonance spectra that are commonly used for backbone assignment, i.e., CBCA(CO)NNH (*9*), CBCANNH (or HNCACB) (*10, 11*), and CC(CO)NNH-TOCSY (*12, 13*). Based on these spectra, spin systems of amino acids are linked together to subsequences and then matched to the protein sequence to obtain the sequence-specific assignment. Usually this is done by identifying amino acids using their C^{α}/C^{β} chemical shifts. In addition, the amino acid types can be distinguished via the topology of the side chain. This is the strategy presented here and amino acids types are conveniently detected by creating selective "fingerprints", i.e., by recording amino acid type-selective ^{1}H–^{15}N correlations.

Schemes for obtaining amino acid type-selective spectra have already been proposed. They achieve the selection either by using a selective pulses (*14–18*) or by exploiting the number of coupling partners with an appropriate tuning of delays (*19–33*). Here, a set of 12 new pulse sequences is presented that result in amino acid type-selective ^{1}H–^{15}N correlations. The new sequences are based on the selection of coherence order via multiple quantum filters and offer a superior suppression of unwanted signals. Sequences are designed to identify the residue type itself as well as residues in the (i + 1) position.

RESULTS

The new experiments all select the signals of the desired amino acid types based on the topology of the side chain. The flow of magnetization that is required to detect certain amino acid types with the new sequences is depicted in Fig. 1. The initial step is the selection of a particular group (NH_2, CH_2, or CH_3) with MUSIC (multiplicity selective in-phase coherence transfer) (*34, 35*). After the selection the magnetization is transferred along the side chain to the C^{α}. From there it is relayed either via the carbonyl carbon to the (i + 1) nitrogen or directly to both nitrogens coupled to the C^{α} (i or i + 1). The signal is finally detected on the amide proton.

The MUSIC pulse sequence elements have recently been proposed (*34, 35*): they are based on the phase-shifted DEPT (*36*) and the POMMIE sequence (*37, 38*) and accomplish an in-phase transfer of magnetization for either XH_2 or XH_3 (X can be ^{15}N or ^{13}C). The sequences used here are shown in Fig. 2 together with the relevant coherence transfer pathways for

[1] To whom correspondence should be addressed. Fax: +49-30-51551-235. E-mail: schmieder@fmp-berlin.de.

1090-7807/99 $30.00

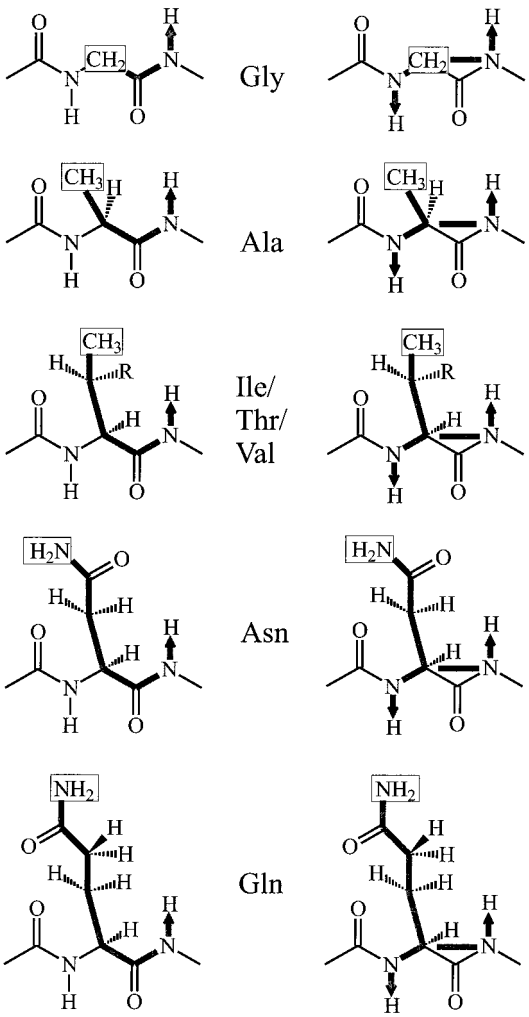

FIG. 1. Schematic representation of the magnetization pathway selected by the new experiments. First a particular group (NH_2, CH_2, or CH_3, indicated by the hatched rectangle) is selected with the MUSIC sequence. From there the magnetization is transferred along the side chain to the C^α carbon and finally to the amide proton, as indicated by the thick lines. The two types of pulse sequences differ in the transfer from the C^α to the nitrogen. In the left column the flow of magnetization in the $(i + 1)$-HSQCs is depicted from the C^α to the carbonyl and then to the nitrogen and amide proton. The right column represents the $(i, i + 1)$-HSQCs, where the magnetization flows from the Cα to either the nitrogen of the same amino acid or that of the $(i + 1)$ neighbor.

protons; the coherence pathway for carbon is trivial and has been omitted for the sake of clarity. The suppression of unwanted multiplicities is based on the creation of multiple quantum coherence and their selection by phase cycling, i.e., by using a multiple quantum filter. Two types of phase cycle may be employed, selecting either XH_2 or XH_3 via a double or a triple quantum filter, respectively. Alternatively pulsed field gradients could be used for coherence selection but would create longer pulse sequences with reduced sensitivity. Placing three gradients of equal length and sign in the three delays of the MUSIC sequence, however, results in an increased performance. Spurious signals from "wrong" amino acids are completely removed, beside a generally better suppression of artifacts.

Since all triple-resonance experiments begin and end with a coherence transfer from and to protons, MUSIC can be implemented in a variety of techniques replacing the INEPT step at the beginning or at the end. An advantage of the new sequences is the superior selection that can be obtained by separating coherence orders, rather than adjusting delays to the size of coupling constants. The latter approach will lead to signals from other amino acids if the coupling constants differ in the various amino acids. The multiple quantum filters used here are also combined with the use of selective pulses that can further help to differentiate between types of amino acids based on characteristic carbon chemical shifts. Another advantage com-

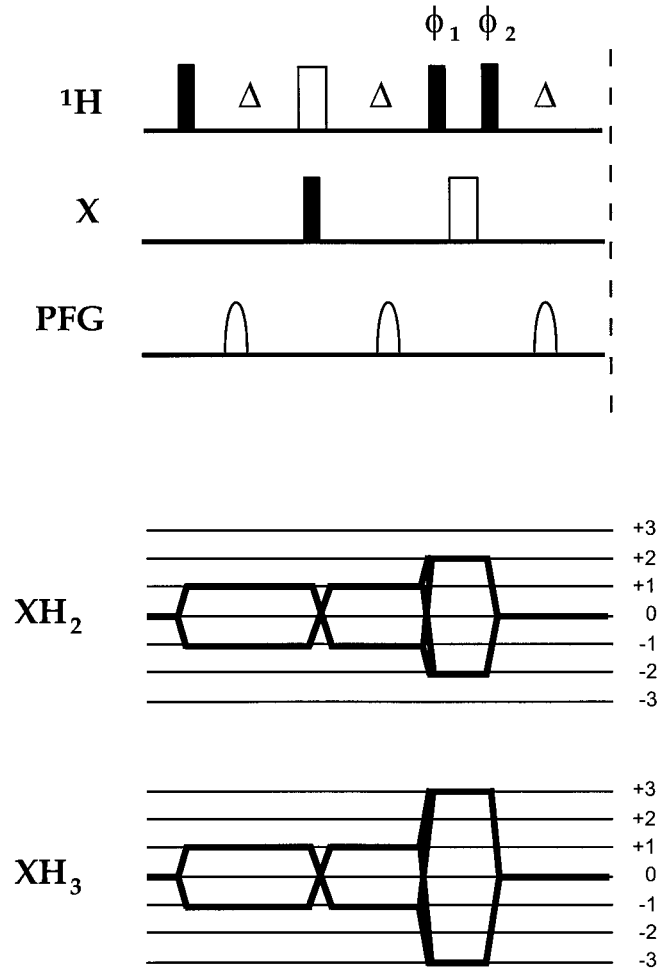

FIG. 2. Pulse sequence and coherence pathway diagram for the MUSIC step used here. The coherence pathway for carbon is trivial and is omitted for the sake of clarity. The phase cycle for the selection of XH_2 is: $\phi_1 = 0°$, $\phi_2 = 45°, 135°, 225°, 315°$, $\phi_{rec} = 0°, 180°$; for the selection of XH_3 it is: $\phi_1 = 0°$, $\phi_2 = 30°, 90°, 150°, 210°, 270°, 330°$, $\phi_{rec} = 0°, 180°$. This phase cycle can be combined with the conventional phase cycling used in the standard triple-resonance experiments. The delays are $\Delta = 5.5$ ms for NH_2 and $\Delta = 3.6$ ms for $CH_{2/3}$. To further improve the performance of sequences three gradients of equal sign and strength are implemented in each of the three delays.

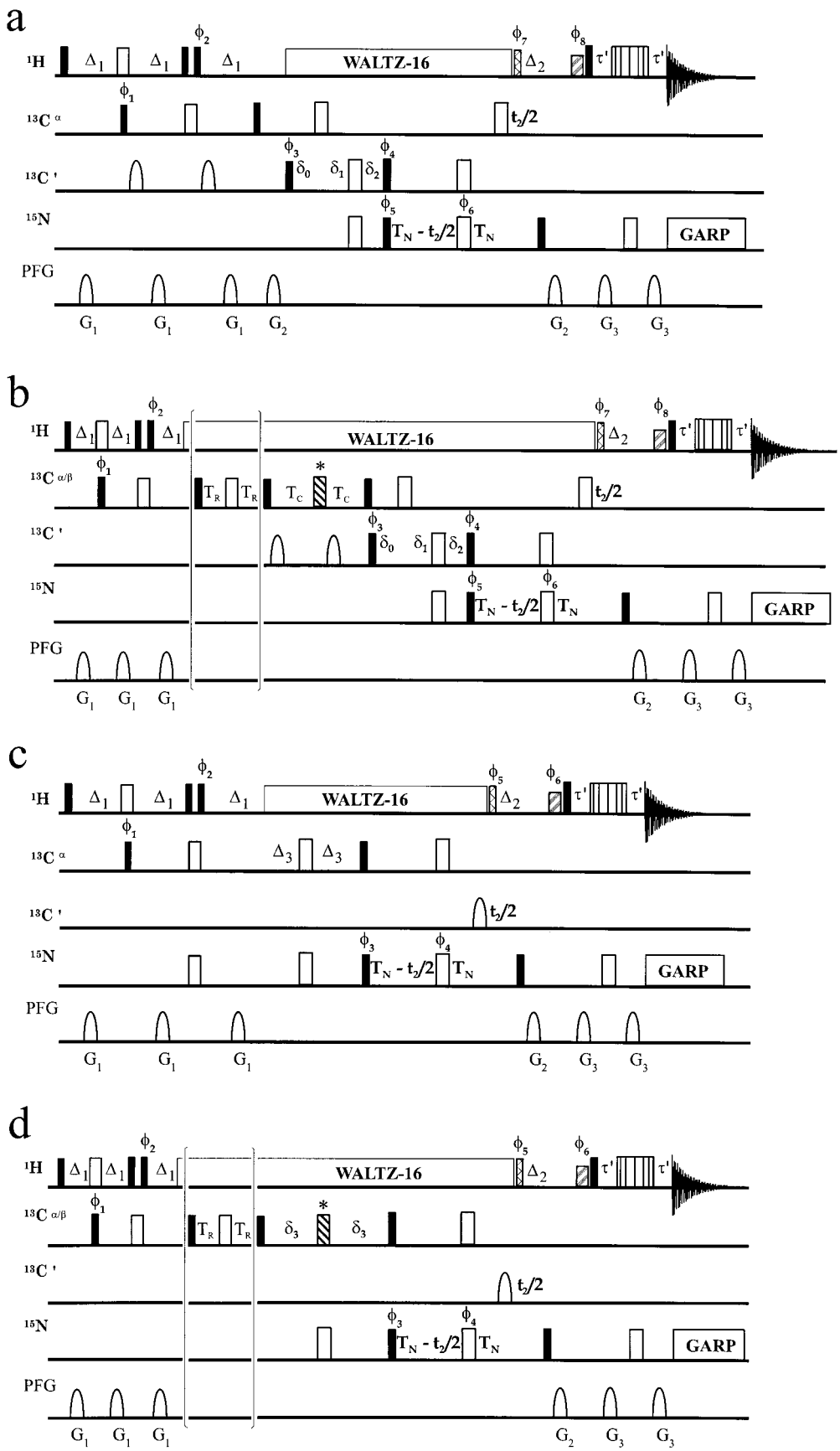
a
b
c
d
WALTZ-16
GARP
PFG

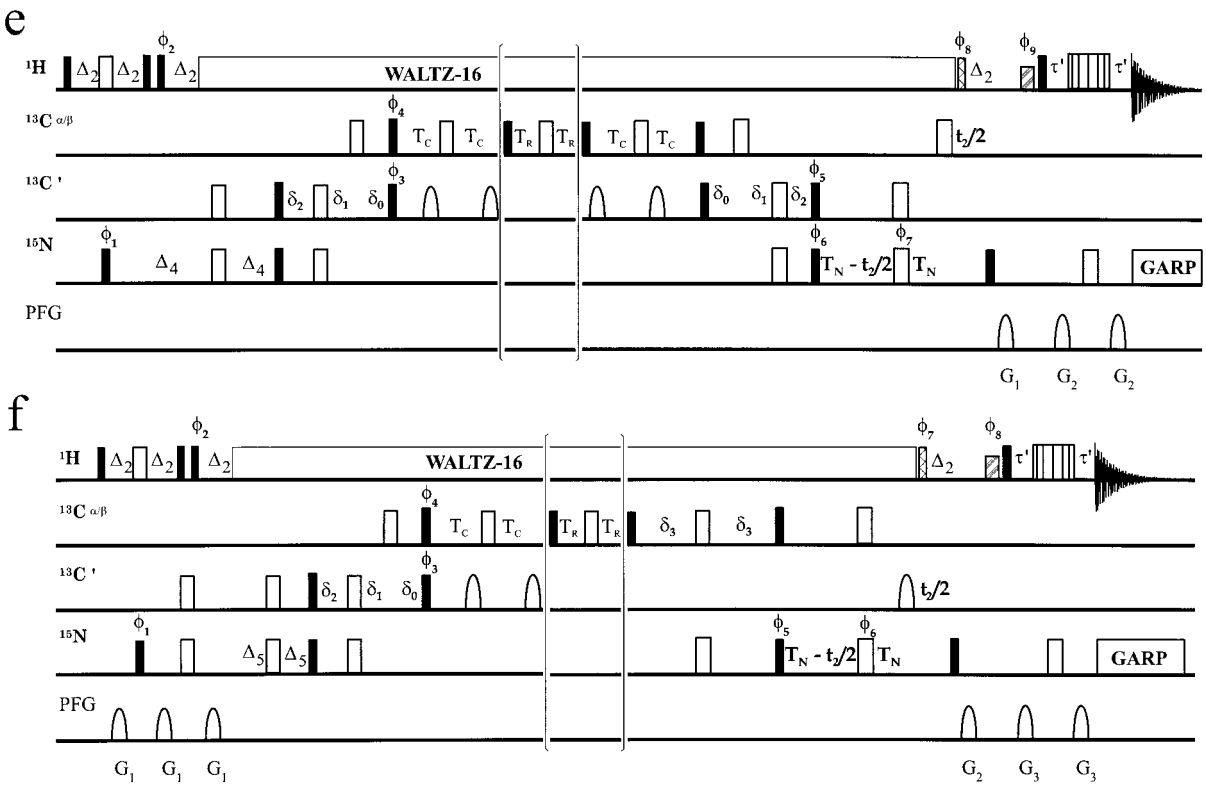

FIG. 3. Pulse sequences of the new amino acid type-selective ^{1}H–^{15}N correlations. The pulse sequences yield spectra for Gly (a and c), Ala, Thr, Ile, and Val (b and d), and Asn and Gln (e and f). Pulses of 90° and 180° are represented by thin black filled and thick unfilled bars, respectively. The water-selective 90° ^{1}H flip-back pulse is represented by a striped thick bar; a hatched thin bar stands for a 90° flip-back ^{1}H pulse at the end of the ^{1}H-decoupling sequence. Magnetic field gradients as well as shaped 180° ^{13}CO pulses are represented by sine shapes. Pulses applied at the $^{13}C^{\alpha}$, $^{13}C^{\alpha/\beta}$, or ^{13}CO resonance frequencies were adjusted to provide a null at the corresponding ^{13}CO or $^{13}C^{\alpha}$ frequencies. The square $^{13}C^{\alpha}$ 90° and 180° pulses were set to 54 and 48 μs, respectively. The square $^{13}C^{\alpha/\beta}$ 90° and 180° pulses were set to 49 and 44 μs, respectively. The square ^{13}CO 90° and 180° pulses were set to 54 and 108 μs, respectively. The shaped 180° ^{13}CO were applied as G3 Gaussian cascade (*50*) with a duration of 256 μs. In the Thr/Ala experiments (b) and (d) the striped thick bar with an asterix stands for a band-selective 180° REBURP pulse (*51*) at 68.5 ppm with a duration of 1024 μs, while this pulse was applied as a normal square 180° pulse in all the other experiments. Unless indicated otherwise, pulses are applied with phase x. Proton hard pulses were applied with 25 kHz field strength; WALTZ-16 (*52*) of ^{1}H spins was achieved using a field strength of 3.1 kHz. The same field strength was used for the subsequent 90° flip-back ^{1}H pulse. The water-selective 90° square pulse had a duration of 1 ms. GARP-1 decoupling (*53*) of ^{15}N was achieved using a field strength of 830 Hz. Water suppression was obtained using WATERGATE implemented with a 3–9–19 pulse (*54*). The gradients were applied as a sinusoidal function from 0 to π. The carrier frequencies were centered at ^{1}H = 4.8 ppm, ^{15}N = 119.6 ppm, $^{13}C^{\alpha}$ = 55 ppm, $^{13}C^{\alpha/\beta}$ = 45 ppm, and ^{13}CO = 175 ppm. The following delays were used: Δ_1 = 3.5 ms, Δ_2 = 5.5 ms, Δ_3 = 7.0 ms, Δ_4 = 13.5 ms, Δ_5 = 8.0 ms, δ_0 = 4.5 ms, δ_1 = 6.9 ms, δ_2 = 11.4 ms, δ_3 = 9.3 ms, T_N = 11 ms, τ' = 2.25 ms, T_R = 4.5 ms (except for the TAVI-experiments where T_R = 3.7 ms), T_C = 4.5 ms. To achieve quadrature detection in the indirect dimension the States-TPPI-States protocol (*55*) was used in all experiments. All spectra were processed using XWINNMR (Bruker AG). (a) G-(i + 1)-HSQC. The phase cycling was: ϕ_1 = 16 (x), 16 ($-x$); ϕ_2 = 2 (45°), 2 (135°), 2 (225°), 2 (315°); ϕ_3 = x, $-x$; ϕ_4 = 50°; ϕ_5 = x; ϕ_6 = 8 (x), 8 (y), 8 ($-x$), 8 ($-y$); ϕ_7 = $-y$; ϕ_8 = $-x$; ϕ_{rec} = 2 (x, 2 ($-x$), x), 4 ($-x$, 2 x, $-x$), 2 (x, 2 ($-x$), x). States-TPPI phase cycling was applied to ϕ_5. Gradients had the following duration and strength: G_1 = 800 μs (7 G/cm), G_2 = 900 μs (28 G/cm), G_3 = 1 ms (21 G/cm). (b) A-(i + 1)-HSQC (omitting the part in parentheses), TAVI-(i + 1)-HSQC (including the part in parentheses and using a normal $^{13}C^{\alpha/\beta}$ 180° pulse (*)), and TA-(i + 1)-HSQC (including the part in parentheses and using a Thr-C^{β}-selective 180° REBURP pulse (*) at 68.5 ppm).The phase cycling was: ϕ_1 = 24 (x), 24 ($-x$); ϕ_2 = 2 (30°), 2 (90°), 2 (150°), 2 (210°), 2 (270°), 2 (330°); ϕ_3 = x, $-x$; ϕ_4 = 50°; ϕ_5 = x; ϕ_6 = 12 (x), 12 (y), 12 ($-x$), 12 ($-y$); ϕ_7 = $-y$; ϕ_8 = $-x$; ϕ_{rec} = 3 (x, 2 ($-x$), x), 6 ($-x$, 2 (x), $-x$), 3 (x, 2 ($-x$), x). States-TPPI phase cycling was applied to phase ϕ_5. The gradients had the following duration and strength: G_1 = 800 μms (7 G/cm), G_2 = 800 μms (28 G/cm), G_3 = 1 ms (21 G/cm). (c) G-(i, i + 1)-HSQC. The phase cycling was: ϕ_1 = x, $-x$; ϕ_2 = 2 (45°), 2 (135°), 2 (225°), 2 (315°); ϕ_3 = 8 (x), 8 ($-x$); ϕ_4 = 4 (x), 4 (y), 4 ($-x$), 4 ($-y$); ϕ_5 = 4 ($-y$), 4 (y); ϕ_6 = ($-x$); ϕ_{rec} = x, 2 ($-x$), x, 2 ($-x$, 2 (x), $-x$), x, 2 ($-x$), x. States-TPPI phase cycling was applied to phase ϕ_3. The gradients had the following duration and strength: G_1 = 1 ms (7 G/cm), G_2 = 800 μs (28 G/cm), G_3 = 1 ms (21 G/cm). (d) A-(i, i + 1)-HSQC (omitting the part in parentheses), TAVI-(i, i + 1) (including the part in parentheses and using a normal $^{13}C^{\alpha/\beta}$ 180° pulse (*)), and TA-(i, i + 1)-HSQC (with the part in parentheses and a Thr-C^{β}-selective 180° REBURP pulse (*) at 68.5 ppm). The phase cycling was: ϕ_1 = 24 (x), 24 ($-x$); ϕ_2 = 2 (30°), 2 (90°), 2 (150°), 2 (210°), 2 (270°), 2 (330°); ϕ_3 = x, $-x$; ϕ_4 = 12 (x), 12 (y), 12 ($-x$), 12 ($-y$); ϕ_5 = $-y$; ϕ_6 = $-x$; ϕ_{rec} = 3 (x, 2 ($-x$), x), 6 ($-x$, 2 (x), $-x$), 3 (x, 2 ($-x$), x). States-TPPI phase cycling was applied to phase ϕ_3. The gradients had the following duration and strength: G_1 = 800 μs (7 G/cm), G_2 = 800 μs (28 G/cm), G_3 = 1 ms (21 G/cm). (e) N-(i + 1)-HSQC (omitting the part in parentheses) and QN-(i + 1)-HSQC (including the part in parentheses). The phase cycling was as follows: ϕ_1 = 16 (x), 16 ($-x$); ϕ_2 = 2 (45°), 2 (135°), 2(225°), 2(315°); ϕ_3 = 310°, ϕ_4 = 32 (x), 32 ($-x$); ϕ_5 = 50°; ϕ_6 = x, $-x$; ϕ_7 = 8 (x), 8 (y), 8 ($-x$), 8 ($-y$); ϕ_8 = 4 ($-y$), 4 (y); ϕ_9 = $-x$; ϕ_{rec} = 2 (x, 2 ($-x$), x), 4 ($-x$, 2 (x), $-x$), 2 (x, 2 ($-x$), x), 2 ($-x$, 2 (x), $-x$), 4 (x, 2 ($-x$), x), 2 ($-x$, 2 (x), $-x$). States-TPPI phase cycling was applied to phase ϕ_6. The

pared to some of the other amino-acid-selective sequences is that the implementation of MUSIC does not lengthen the sequence compared to the standard triple-resonance experiments. Therefore no loss of intensity due to relaxation is observed. The creation of proton double quantum coherence in the selection of XH_2 is 100% effective and no reduction of intensity is visible in those spectra compared to the standard triple-resonance experiments. The creation of proton triple quantum coherence is only 50% effective and the intensity is reduced by a factor of 2 compared to the standard triple-resonance experiments. This has been confirmed experimentally (data not shown). The time required to record the amino-acid-selective correlations with sufficient intensity is therefore only in the range of some hours. It should be noted that a peak missing in a less sensitive experiment is a minor problem in the context of automated assignment, compared to the problem of the occurrence of spurious peaks from residues that have not been properly suppressed.

We present here 12 different pulse sequences. Six of them represent the $(i + 1)$ version and the other 6 the $(i, i + 1)$ version of an amino acid type-selective ^1H–^{15}N correlation. In analogy to the conventional triple-resonance experiments the latter experiments will be somewhat less sensitive and can potentially contain two signals per residue of which the $(i + 1)$ will be weaker. They are applied to two different protein domains, the SH3 domain from spectra (*39*) and the SAM domain from EphB2 (*40, 41*).

Gly

Glycine is the only amino acid that has a methylene group in the C^α position. The implementation of a CH_2 selection into the CA(CO)NNH (*42*) and the CANNH (*43*) therefore leads to a selection of the Gly side chain (Fig. 2). The pulse sequences of the G-$(i + 1)$-HSQC and the G-$(i, i + 1)$-HSQC are given in Figs. 3a and 3c, respectively. The corresponding two-dimensional spectra are shown in Figs. 5a and 5b. A similar pattern as that of Gly may be found in the Asn and Gln side chain with respect to the CA(CO)NNH experiment and in Arg with respect to the CANNH experiment. Since the delay for magnetization transfer from the nitrogen to the amino proton is chosen to be $(2J_{NH})^{-1}$, the signals involving side chain nitrogens of Asn and Gln should not show up. The spectra are recorded in 90% H_2O/10% D_2O, however, and some signals from the NHD groups in their side chains will be visible. Since side chain amide groups are easily distinguished or identified with a separate experiment (*44*), this will not affect the information content of the spectra. The same is true for the Arg side chain signals that will show up in the $(i, i + 1)$ experiment. They can easily be identified in a conventional HSQC based on their chemical shift.

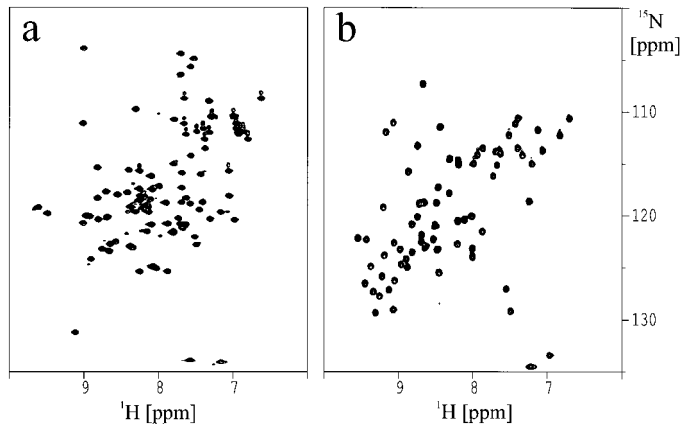

FIG. 4. ^{15}N-HSQC of the two protein domains used for the new experiments. The spectra are given as a comparison for the spectra from the new selective experiments (Figs. 5 to 7). (a) HSQC of the SAM domain from EphB2, a protein of 83 residues; (b) HSQC of the SH3 domain from spectrin, a protein of 62 residues.

Ala

Alanine-selective experiments are created by implementing a selection of CH_3 groups in the CBCA(CO)NNH (*9*) and the CBCANNH (*10*). Since alanine is the only amino acid with a methyl group in the β-position (Fig. 1), it is the only type of amino acid whose coherences can pass through the experiment. The pulse sequence of the A-$(i + 1)$-HSQC and the A-$(i, i + 1)$-HSQC are shown in Figs. 3b and 3d and the spectra in Figs. 5c and 5d.

Thr, Ala, Val, Ile (TAVI)

The Ala experiment may be extended by a RELAY step. In this case the amino acids that have a methyl group in the γ-position are selected. Those are Thr, Val, and Ile (Fig. 1). Signals from alanine will also be present in the spectrum since the RELAY sequence does not suppress magnetization that is not transferred in the final step before the transfer to carbonyl or nitrogen. These signals can, however, easily be distinguished with the experiment mentioned before. The pulse sequence of the TAVI-$(i + 1)$-HSQC and the TAVI-$(i, i + 1)$-HSQC are shown in Figs. 3b and 3d and the spectra in Figs. 6a and 6b. An experiment to select Thr, Val, and Ile has been proposed before, utilizing the fact that the β-position is a CH

gradients had the following duration and strength: $G_1 = 800$ μs (28 G/cm), $G_2 = 1$ ms (21 G/cm). (f) N-$(i, i + 1)$-HSQC (omitting the part in parentheses) and QN-$(i, i + 1)$-HSQC (including the part in parentheses). The phase cycling was: $\phi_1 = 16\ (x), 16\ (-x)$; $\phi_2 = 2\ (45°), 2\ (135°), 2\ (225°), 2\ (315°)$; $\phi_3 = 310°$, $\phi_4 = 32\ (x), 32\ (-x)$; $\phi_5 = x, -x$; $\phi_6 = 8\ (x), 8\ (y), 8\ (-x), 8\ (-y)$; $\phi_7 = 4\ (-y), 4\ (y)$; $\phi_8 = -x$; $\phi_{rec} = 2\ (x, 2\ (-x), x), 4\ (-x, 2\ (x), -x), 2\ (x, 2\ (-x), x), 2\ (-x, 2\ (x), -x), 4\ (x, 2\ (-x), x), 2\ (-x, 2\ (x), -x)$. States-TPPI phase cycling was applied to phase ϕ_5. The gradients had the following duration and strength: $G_1 = 800$ μs (7 G/cm), $G_2 = 800$ μs (28 G/cm), $G_3 = 1$ ms (21 G/cm).

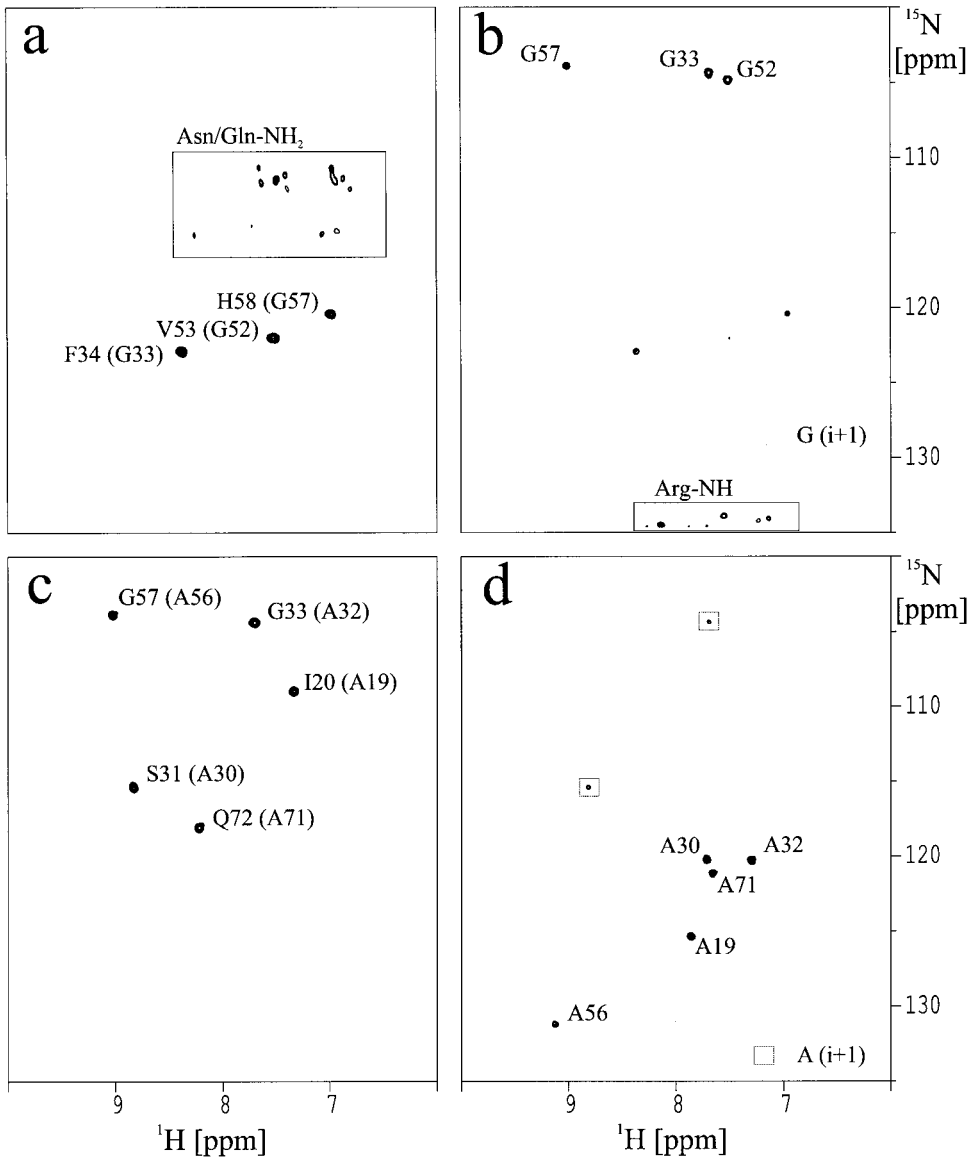

FIG. 5. Amino acid type-selective ^{1}H–^{15}N correlations of the SAM domain from EphB2. (a) The G-(i + 1)-HSQC was acquired in 25 min using 8 scans per complex point. The SAM domain contains three glycines which results in three strong signals from sequential neighbors of Gly. Weak signals from the Asn and Gln are present, which are due to NDH groups (see text). (b) The G-(i, i + 1)-HSQC was acquired in 50 min using 16 scans per complex point. In addition to the three signals of the Gly residues the sequential neighbors are also present with weak intensity. They are marked with small rectangles. Arg $N^{\epsilon}H^{\epsilon}$ peaks also appear in the spectrum (see text). These peaks are weaker and distorted since Arg C^{δ} is not in the chemical shift range covered by the semiselective pulses. (c)/(d) The A-(i + 1)-HSQC and the A(i, i + 1)-HSQC were acquired in 2 h 15 min each using 48 scans per complex point. The SAM domain contains five alanines. In the (i + 1) experiment (c) the expected five signals from sequential neighbors of Ala are present. In the (i, i + 1) experiment (d) all five Ala residues show strong signals while two weak signals result from amino acids in the (i + 1) position of the alanine residues. They are marked with small rectangles.

(*27*). As already pointed out, the new experiment is cleaner, since the selection via coherence order is less sensitive to variations in the size of the coupling constant.

Thr, Ala (TA)

The TAVI sequence can be modified using a selective pulse to distinguish Thr and Ala from Val and Ile. This pulse replaces the semiselective pulse in the delay for the transfer of magnetization from the C^{α} to the carbonyl or the nitrogen in the (i + 1) and (i, i + 1) sequence, respectively. At the beginning of that delay, the magnetization of Thr, Val, and Ile has just been transferred to C^{α} and the C^{β} is anti-phase with respect to the C^{α}. The Thr-C^{β} chemical shifts are similar to those of the α-carbons and a selective pulse affecting only this region will prevent the creation of detectable magnetization for Val and Ile since the coupling from the C^{β} to the C^{α} cannot be

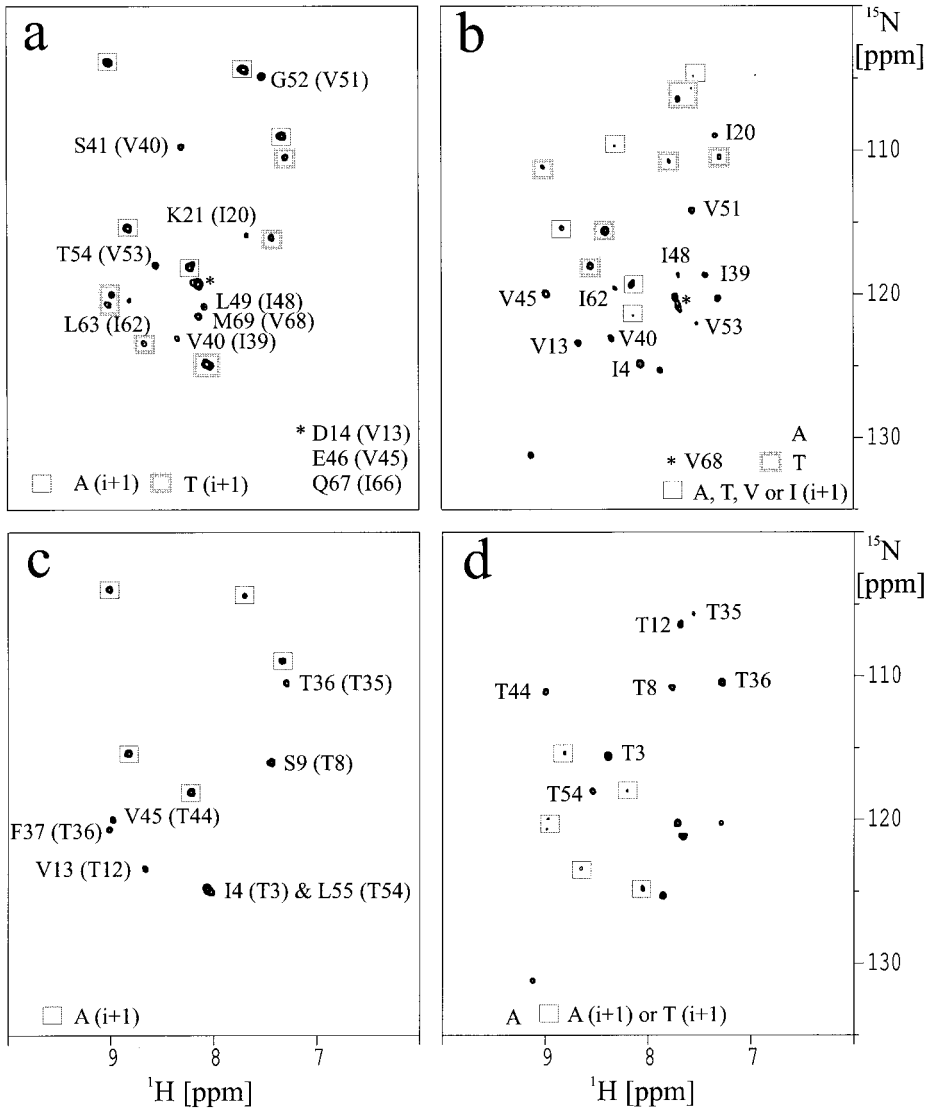

FIG. 6. Amino acid type-selective ^{1}H–^{15}N correlations of the SAM domain from EphB2. (a) The TAVI-(i + 1)-HSQC was acquired in 2 h 15 min using 48 scans per complex point. (b) The TAVI-(i, i + 1)-HSQC was acquired in 4 h 30 min using 96 scans per complex point. (c) The TA-(i + 1)-HSQC was acquired in 2 h 15 min using 48 scans per complex point. (d) The TA-(i, i + 1)-HSQC was acquired in 4 h 30 min using 96 scans per complex point. The SAM domain contains 7 threonines, 6 isoleucines, and 6 valines. In the TAVI-(i + 1)-HSQC (a) all 18 expected signals appear (only 5 Ile can appear since Ile-4 has a proline as a sequential neighbor). The 7 sequential neighbors of Thr are marked with thick rectangles. Five sequential neighbors of Ala also appear (marked with thin rectangles) but can easily be identified using the A-(i + 1)-HSQC (Fig. 5c). In the TAVI-(i, i + 1)-HSQC (b) signals from all 7 Thr are marked with thick dark rectangles; all signals from Val and Ile except that of I66 are also visible. Again signals from alanine appear (marked with thick light rectangles) that can easily be identified (Fig. 5d). In the TA-(i + 1)-HSQC (c) signals from sequential neighbors of all 7 Thr and all 5 Ala (marked with rectangles) are present, while signals from Ile and Val are suppressed. Finally, in the TA-(i, i + 1)-HSQC (d) again all Thr and all Ala signals (marked with thick light rectangles) are visible. The rest of the signals are signals from sequential neighbors of Ala or Thr and can be identified by comparison with the TA-(i + 1)-HSQC. The (i + 1) peaks are marked with thin rectangles.

refocused. In alanine the magnetization is already transferred to the C^{α} and the coupling already refocused at the beginning of that delay. Thus the selective pulse will only prevents loss of intensity due to the evolution of coupling to the C^{β}. The pulse sequences of the TA-(i + 1)-HSQC and the TA-(i, i + 1)-HSQC are also shown in Figs. 3b and 3d and the resulting spectra in Figs. 6c and 6d.

Asn, Gln

MUSIC can also be used to select NH_2 groups. In combination with a transfer to the carbonyl carbon this yields a selection of Asn and Gln (*34*). From the carbonyl carbon the magnetization can then be transferred to the C^{α} and then further as described above to yield (i + 1) or (i, i + 1) spectra

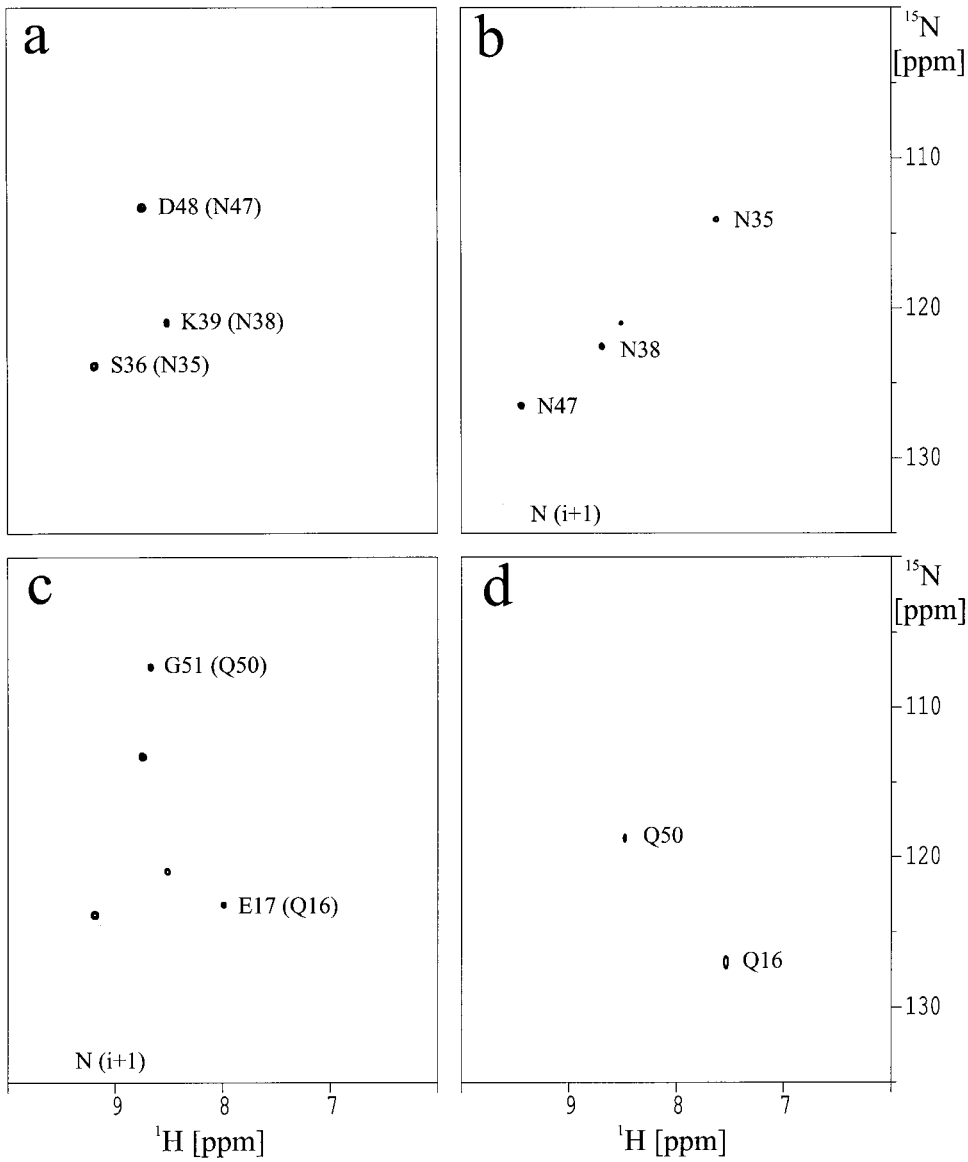

FIG. 7. Amino acid type-selective ^{1}H–^{15}N correlations of the SH3 domain from spectrin. The SH3 domain contains three asparagines and two glutamines. (a) The N-(i + 1)-HSQC was acquired in 3 h using 64 scans per complex point. All three expected signals are visible. (b) The N-(i, i + 1)-HSQC was acquired in 4 h 30 min using 96 scans per complex point and contains all three Asn residues. The other peak marked with a rectangle is a signal from K39, i.e., a signal from a sequential neighbor. (c) The QN-(i + 1)-HSQC was acquired in 4 h 30 min using 96 scans per complex point. It contains the five possible signals; the three signals from Asn are marked with rectangles. (d) The QN-(i, i + 1)-HSQC was acquired in 6 h using 128 scans per complex point and contains only the two signals from Gln. Signals from Asn are too weak to be detectable.

(Fig. 2). In the case of Asn this takes a simple COSY step; in the case of the Gln an additional RELAY step is necessary. Signals from Asn will also show up in the Gln experiment, but since the experiment is optimized for Gln their intensity can be close to zero (see Fig. 7d). The pulse sequences of the N-(i + 1)-HSQC, the N-(i, i + 1)-HSQC, the NQ-(i + 1)-HSQC, and the NQ-(i, i + 1)-HSQC are shown in Figs. 3e and 3f. They are in part similar to the HN(COCA)CB (*45*) and the HN(COCACB)CG (*46*) sequences. The spectra are shown in Figs. 7a to 7d. Note that sequences which select NH_2 groups will also be applicable in situations where the protein has been deuterated. In that case the delays to transfer the magnetization along the side chain can be extended to the full length of $(2J_{CC})^{-1}$ since almost no loss of intensity due to relaxation will occur and a more efficient transfer via the carbon–carbon couplings is possible.

The delays used for the transfer of magnetization in all of the new sequences were optimized using the delays from the standard experiments as a starting point. The situation in the selective experiments is, however, different from that in the standard experiments. The signal that is finally detected does not result from all protons of the amino acid. Only magneti-

zation from protons selected by the MUSIC sequence is transferred along the side chain. In the standard sequences delays are often tuned to $(4J_{CC})^{-1}$ to account for the fact that antiphase magnetization has to be refocused while in-phase magnetization should not be defocused during the same delay. This restriction does not apply for most of the delays in the new pulse sequences presented here and delays can usually be chosen to be longer than $(4J_{CC})^{-1}$. Only the delay T_R in the TAVI experiment has the standard value, since otherwise the passive coupling of the C^{β} to the other C^{γ} in Val and Ile would reduce the intensity. In the other sequences a longer T_R reduces the intensities of those peaks already identified in other spectra (Ala in the TA-HSQCs and Asn in NQ-HSQCs).

If the delays are chosen to be longer, however, loss due to relaxation can occur. The delays given in Fig. 3 were optimized experimentally using two protein domains of 62 (SH3) and 83 (SAM) amino acids and are longer than in the standard sequences. For larger proteins is might be necessary to reduce the length of the delays back to the original values.

CONCLUSION

We have presented a set of new pulse sequences that yield amino acid type-selective ^{1}H–^{15}N correlations. The resulting novel two-dimensional spectra may be used in addition to the conventional three-dimensional spectra and will take only a small amount of spectrometer time. The clean selection possible with these sequences should make an automated assignment easier, especially if the conventional three-dimensional spectra are crowded and less than perfect. The concept used here to create amino acid type-selective ^{1}H–^{15}N correlations can be transferred to the family of the HCACO-COSY sequences (*47–49*) to yield amino acid type-selective ^{1}H–^{13}C correlations. Those spectra can then supplement the side chain assignment based on HCCH-type sequences. Further sequences that select other types of amino acids will be presented elsewhere; in particular a more refined use of selective pulses will permit more experiments.

EXPERIMENTAL

The spectra were recorded on a DRX600 in standard configuration using an inverse triple-resonance probe equipped with three-axis self-shielded gradient coils. Two different protein domains were used for the experiments. The Asn/Gln experiments were recorded with a 0.8-mM sample of the SH3 domain labeled with ^{15}N and ^{13}C. For all other experiments a 1.5-mM sample of the SAM domain from EphB2 labeled with ^{15}N and ^{13}C was used. For both samples 5-mm ultraprecision sample tubes were used. The HSQC spectra of both domains are shown in Fig. 4 as a comparison for the spectra shown in Figs. 5, 6, and 7. The HSQC of the SAM domain (Fig. 4a) was recorded with 512 complex points in each dimension, a spectral width of 3012 Hz (^{15}N) $\times$ 10000 Hz (^{1}H), and 8 transients. All other spectra were recorded in an identical way but with 64 (t_1) $\times$ 512 (t_2) complex points. The data were processed using a squared sine bell shifted by 90° as a window function in both dimensions. The ^{15}N t_1 interferograms were quadrupled in length by linear prediction using XWINNMR, except for the spectrum of the SAM domain. The final spectrum had a size of 512 (t_1) $\times$ 1024 (t_2) real points.

ACKNOWLEDGMENTS

Support from the Forschungsinstitut für Molekulare Pharmakologie is gratefully acknowledged. Mario Schubert is supported by the DFG Graduiertenkolleg GRK 80 "Modellstudien." Peter Schmieder thanks the Fonds der chemischen Industrie for a fellowship (Liebig Li 150/9 SZ). The authors thank Wolfgang Bermel and Rüdiger Winter for helpful discussions and the assignment of the SH3 domain and Martina Leidert for the preparation of the SH3 sample. The work was supported by a grant of the BMBF (01 GG 9812, Leitprojekt "Proteinstrukturfabrik").

REFERENCES

1. G. T. Montelione and G. Wagner, *J. Magn. Reson.* **87,** 183 (1990).
2. L. E. Kay, M. Ikura, R. Tschudin, and A. Bax, *J. Magn. Reson.* **89,** 496 (1990).
3. D. E. Zimmerman and G. T. Montelione, *Curr. Opin. Struct. Biol.* **5,** 664 (1995) and references cited therein.
4. K. B. Li and B. C. Sanctuary, *J. Chem. Inf. Comput. Sci.* **37,** 359 (1997).
5. K. B. Li and B. C. Sanctuary, *J. Chem. Inf. Comput. Sci.* **37,** 467 (1997).
6. D. E. Zimmerman, C. A. Kulikowski, Y. Huang, W. Feng, M. Tashiro, S. Shimotakahara, Ch. Chien, R. Powers, and G. T. Montelione, *J. Mol. Biol.* **269,** 592 (1997).
7. D. Croft, J. Kemmink, K.-P. Neidig, and H. Oschkinat, *J. Biomol. NMR* **10,** 207 (1997).
8. M. Leutner, R. M. Gschwind, J. Liermann, C. Schwarz, G. Gemmecker, and H. Kessler, *J. Biomol. NMR* **11,** 31 (1998).
9. S. Grzesiek and A. Bax, *J. Am. Chem. Soc.* **114,** 6291 (1992).
10. S. Grzesiek and A. Bax, *J. Magn. Reson. B* **99,** 201 (1992).
11. M. Wittekind and L. Mueller, *J. Magn. Reson. B* **101,** 201 (1993).
12. S. Grzesiek, J. Anglister, and A. Bax, *J. Magn. Reson. B* **101,** 114 (1993).
13. T. M. Logan, E. T. Olejniczak, R. X. Xu, and S. W. Fesik, *FEBS Lett.* **314,** 413 (1992).
14. N. S. Rao, P. Legault, D. R. Muhandiram, J. Greenblatt, J. L. Battiste, J. R. Williamson, and L. E. Kay, *J. Magn. Reson. B* **113,** 272 (1993).
15. H. Vis, R. Boelens, M. Mariani, R. Stroop, C. E. Vorgias, K. S. Wilson, and R. Kaptein, *Biochemistry* **33,** 14858 (1994).
16. T. Yamazaki, S. M. Pascal, A. U. Singer, J. D. Forman-Kay, and L. E. Kay, *J. Am. Chem. Soc.* **117,** 3556 (1995).
17. M. Pellecchia, G. Wider, H. Iwai, and K. Wüthrich, *J. Biomol. NMR* **10,** 193 (1997).
18. C. Zwahlen, S. J. F. Vincent, K. H. Gardner, and L. E. Kay, *J. Am. Chem. Soc.* **120,** 4825 (1998).
19. M. Wittekind, W. J. Metzler, and L. Mueller, *J. Magn. Reson. B* **101,** 214 (1993).

20. E. T. Olejniczak and S. W. Fesik, *J. Am. Chem. Soc.* **116,** 2215 (1994).

21. K. Gehring and E. Guittet, *J. Magn. Reson. B* **109,** 206 (1995).

22. M. Tashiro, C. B. Rios, and G. T. Montelione, *J. Biomol. NMR* **6,** 211 (1995).

23. B. T. Farmer II and R. A. Venters, *J. Biomol. NMR* **7,** 59 (1996).

24. W. Feng, C. B. Rios, and G. T. Montelione, *J. Biomol. NMR* **8,** 98 (1996).

25. C. B. Rios, W. Feng, M. Tashiro, Z. Shang, and G. T. Montelione, *J. Biomol. NMR* **8,** 345 (1996).

26. V. Dötsch, R. E. Oswald, and G. Wagner, *J. Magn. Reson. B* **110,** 107 (1996).

27. V. Dötsch, R. E. Oswald, and G. Wagner, *J. Magn. Reson. B* **110,** 304 (1996).

28. V. Dötsch, and G. Wagner, *J. Magn. Reson. B* **111,** 310 (1996).

29. V. Dötsch, H. Matsuo, and G. Wagner, *J. Magn. Reson. B* **112,** 95 (1996).

30. F. Löhr and H. Rütherjans, *J. Magn. Reson.* **124,** 255 (1997)

31. M. Pellecchia, H. Iwai, T. Szyperski, and K. Wüthrich, *J. Magn. Reson.* **124,** 274 (1997).

32. D. R. Muhandiram, P. E. Johnson, D. Yang, O. Zhang, L. P. McIntosh, and L. E. Kay, *J. Biomol. NMR* **10,** 283 (1997).

33. R. Bazzo, D. O. Cicero, and G. Barbato, *J. Magn. Reson.* **136,** 15 (1999).

34. P. Schmieder, M. Leidert, M. Kelly, and H. Oschkinat, *J. Magn. Reson.* **131,** 199 (1998).

35. P. Schmieder, M. Smalla, and H. Oschkinat, *in* "Proceedings of the 29. AMPERE - 13. ISMAR International Conference on Magnetic Resonance and Related Phenomena," (D. Ziessow and W. Lubitz, Eds.) Berlin, 134 (1998).

36. M. Levitt and R. R. Ernst, *Mol. Phys.* **50,** 1109 (1983).

37. J. M. Bulsing, W. M. Brooks, J. Field, and D. M. Doddrell, *J. Magn. Reson.* **56,** 167 (1984).

38. J. M. Bulsing, W. M. Brooks, J. Field, and D. M. Doddrell, *Chem. Phys. Lett.* **104,** 229 (1984).

39. F. J. Blanco, A. R. Ortiz, and L. Serrano, *J. Biomol. NMR* **9,** 347 (1997).

40. C. P. Ponting, *Protein Sci.* **4,** 1928 (1995).

41. M. Smalla, P. Schmieder, M. Kelly, A. ter Laak, G. Krause, L. Ball, M. Wahl, P. Bork, and H. Oschkinat, *Protein Sci.,* in press.

42. W. Boucher, E. D. Laue, S. Campbell-Burk, and P. J. Domaille, *J. Am. Chem. Soc.* **114,** 2262 (1992).

43. W. Boucher, E. D. Laue, S. Campbell-Burk, and P. J. Domaille, *J. Biomol. NMR.* **2,** 631 (1992).

44. J. M. Schmidt and H. Rüterjans, *J. Am. Chem. Soc.* **112,** 760 (1990).

45. T. Yamazaki, W. Lee, C. H. Arrowsmith, D. R. Muhandiram, and L. E. Kay, *J. Am. Chem. Soc.* **116,** 11655 (1994).

46. S. A. McCallum, T. K. Hitchen, and G. S. Rule, *J. Magn. Reson.* **134,** 350 (1998).

47. L. E. Kay, M. Ikura, A. A. Grey, and D. R. Muhandiram, *J. Magn. Reson.* **99,** 652 (1992).

48. L. E. Kay, *J. Magn. Reson. B* **101,** 110 (1993).

49. L. E. Kay, *J. Am. Chem. Soc.* **115,** 2055 (1993).

50. L. Emsley and G. Bodenhausen, *Chem. Phys. Lett.* **165,** 469 (1990).

51. H. Geen and R. Freeman, *J. Magn. Reson.* **93,** 93 (1991).

52. A. J. Shaka, J. Keeler, T. Frenkiel, and R. Freeman, *J. Magn. Reson.* **53,** 334 (1983).

53. A. J. Shaka, P. B. Barker, and R. Freeman, *J. Magn. Reson.* **53,** 547 (1985).

54. V. Sklenar, M. Piotto, R. Leppik, and V. Saudek, *J. Magn. Reson. A* **102,** 241 (1993).

55. D. Marion, M. Ikura, R. Tschudin, and A. Bax, *J. Magn. Reson.* **85,** 393 (1989).